

## Critical Failure Strain of Oxide Scale in Boiler Austenitic Tubes

Open  
Access

Yeo Wei Hong<sup>1</sup>, Mohamed Hairol Mohd Ali<sup>2</sup>, Zuruza Abu Samah<sup>2</sup>, Ahmad Syamaizar Ahmad Sabli<sup>2</sup>, Mohd Asri Muhammad<sup>2</sup>, Siti Mazulianawati Majid<sup>2</sup>, Ahmad Shamil Abd Rahman<sup>2</sup>, Judha Purbolaksono<sup>2,\*</sup>

<sup>1</sup> Department of Mechanical and Material Engineering, Universiti Tunku Abdul Rahman, Kuala Lumpur 53300, Malaysia

<sup>2</sup> Mechanical Engineering Program Area, Faculty of Engineering, Universiti Teknologi Brunei, Bandar Seri Begawan BE 1410, Brunei Darussalam

### ARTICLE INFO

#### Article history:

Received 8 March 2018

Received in revised form 12 April 2018

Accepted 13 April 2018

Available online 16 April 2018

#### Keywords:

Austenitic alloy, oxide scale growth, critical failure strain, heat transfer, boiler tubes

### ABSTRACT

Exfoliation of oxide scales is known to be associated with the stress and strain developed during the oxide growth. This paper presents a simple procedure to estimate the oxide scale growths and critical failure strains in boiler austenitic tubes over a period of time. In this work, a classical heat flow formula and the relationship between the Larson Miller Parameter (LMP) and the scale thickness were utilized. An approach called Advance Oxide Scale Failure Diagram (A-OSFD) was adopted. The oxide scale failure diagram would provide a general guidance to the power plant engineers to estimate the critical strains. The technique may be used as a supplementary condition monitoring tool for oxide scale growths and to evaluate the critical failure strains.

Copyright © 2018 PENERBIT AKADEMIA BARU - All rights reserved

## 1. Introduction

Having a technologically clean energy source, abundant availability and the affordable prices would make coal to be one of the major energy alternatives for oil and gas in the future [1]. Extensive review on the common types of fuels in steam power plants was reported by Khattak *et al.*, [2]. It has also been reported that the ultra-supercritical (USC) boilers that seem more suitable technology for power generation from coal will be generally employed by the power plant operators worldwide [3-6]. However, formation of oxide scales is known to be a problem of nature during the steam power generation operation. As a consequence, the oxide scales may be exfoliated due to the stress and strain developed during the oxide growth. The scale structure which commonly consists of voids can affect the ability of the scales to withstand the strains. In many instances, the exfoliation occurs near the metal-scale interface or at the interface between the outer and inner part of the scale [7]. Armitt *et al.*, [8] introduced an exfoliation mechanism by relating the accumulated elastic strain in oxide scales to the wall thickness to estimate the

\* Corresponding author.

E-mail address: [judha.purbolaksono@utb.edu.bn](mailto:judha.purbolaksono@utb.edu.bn) (Judha Purbolaksono)

tendencies of scale damage and exfoliation. They presented the concept of oxide scale failure diagram (also called Armitt diagram) to define the regimes for various failure modes as a function of strain (in the oxide) and oxide thickness. Although the concept has been reported to be working well in certain material system such as oxide growth in ferritic steels, but it may not produce a desire estimation in other material system [9].

One of the important considerations in the selection of materials for an ultra-supercritical (USC) boiler is steam-side oxidation [10]. Power plants operating at higher steam temperatures would pose the possibility of having higher rates of steam-side oxidation. In a power plant, steam-side oxidation has three potential unfavourable aspects, all of which are worsened at the higher temperatures planned for USC operation: a) the wall thinning can escalate the hoop stress, causing creep rupture, b) the low thermal conductivity as a result of the thickening oxide scale would further insulate the tube material from the cooling fluid, leading to the increase of fireside metal temperature, thus increasing the fire-side and steam-side corrosion rates, c) The thicker oxide scales may more easily spall during the cooling process of the shutdown of the power plant, blocking steam flow or causing erosion damage of the steam turbine [10].

It has been widely reported that the austenitic alloy is one of the available materials suitable for higher temperature applications in power plants [11, 12]. In a relevant work, Kritzer [13] reported phenomena of wet air oxidation and supercritical water oxidation. However, there are relatively few published reports of the systematic collection of data concerning the growth of oxide scales on the steam-side surfaces of austenitic alloys in steam boilers. Sarver and Tanzosh [14] reported an extensive literature review on the oxidation kinetics and the steam oxidation resistance of the candidate materials that could potentially be used in the USC coal power plants where the power plant could be operated up to 760°C and 38 MPa steam conditions. Limited information was found for the alloys of interest at these high temperatures and pressures.

Numerical heat transfer analyses on fluid flows have been well reported in literature. To name a few, the recent heat transfer analyses on different flowing systems were carried out by researchers [15-18]. In this work, a simple procedure utilizing a classical heat flow formula and the relationship between the Larson Miller Parameter (LMP) and the scale thickness proposed by Yeo *et al.*, [19] is used to estimate the oxide scale growth and temperature increase in a given length of alloy tubes for a period of time. Next, a comprehensive approach called Advance Oxide Scale Failure Diagram which was introduced by Schütze *et al.*, [20] is adopted. The A-OSFD approach considers a more comprehensive operational parameter which took into account the contributing factors such as physical defect size, scale thickness, Young's modulus, and fracture toughness. Those factors could affect the critical failure strain. Based on the approaches by Yeo *et al.*, [19] and Schütze *et al.*, [20], a simple procedure may be proposed for estimating the critical failure strain of the oxide in austenitic tubes for a period of time.

## 2. Methodology

### 2.1 Heat transfer theory

In analyzing the steady state heat transfer in boiler tubes (superheater/reheater), forced convections on the inner surface due to the fully-developed turbulent flow of steam and cross flow of the hot flue gas over bare tubes on the outer surface as shown in Fig. 1 are considered. Referring to Fig. 1, the corresponding heat flow  $Q/A$  equation can be written as

$$\frac{Q}{A} = \frac{T_{gas} - T_{steam}}{\frac{r_4}{r_1 \cdot h_s} + \frac{r_4 \cdot \ln(\frac{r_2}{r_1})}{k_s} + \frac{r_4 \cdot \ln(\frac{r_3}{r_2})}{k_m} + \frac{r_4 \cdot \ln(\frac{r_4}{r_3})}{k_s} + \frac{1}{h_g}} \quad (1)$$

where  $r_1$  and  $r_4$  are the radii of the tube,  $T_{gas}$  is the bulk gas temperature,  $h_g$  is the convection coefficient of the flue gas and the bulk temperature  $T_{steam}$ ,  $h_s$  is the convection coefficient of the steam,  $k_m$  and  $k_s$  are the thermal conductivities for metal and oxide scale, respectively, and  $r_2$  and  $r_3$  are the radii at scale/metal interfaces. The sought values in Fig. 1 are the temperatures at the steam-side  $T_1$ , steam-side scale/metal  $T_2$  and metal/fireside scale interfaces  $T_3$ , and fireside  $T_4$ .

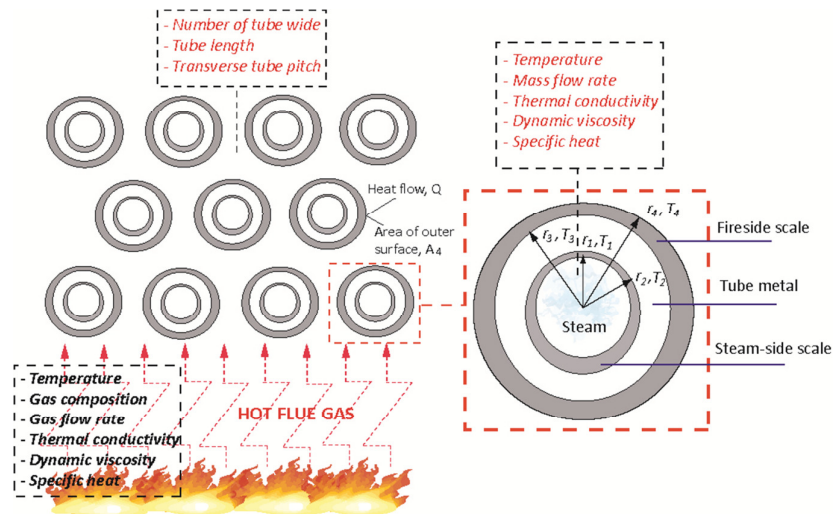


**Fig. 1.** A schematic diagram of heat transfer of staggered boiler tubes and scale formations in steam power plant

## 2.2 Oxide scale data

The data of the LMP versus the scale thickness can be generally approximated in the form of a linear equation as [19]

$$\text{Log}_{10}(X) = C_1 \cdot \text{LMP} - C_2 \quad (2)$$

where the constant  $C_1$  and  $C_2$  are 10.633 and 0.000564, respectively, and  $X$  is the scale thickness in  $\mu\text{m}$ . The Larson-Miller Parameter is a function of time and temperature, where  $T$  is the temperature in Kelvin and  $t$  is the service time in hours ( $h$ ).

The common steam mass flow rate of 3600 kg/h is considered. The operating flue gas temperature of 1200°C and the 50 mm OD (outer diameter) x 10 mm thick tube are used for the simulations. The widely used austenitic steel TP 347HFG is chosen for the simulations.

## 2.3 Physical data

The oxide layers formed in 18% Cr austenitic steel commonly consist of two distinct layers (duplex): an outer layer of essentially pure magnetite and inner layer consisting of a mixture of Fe-Cr spinel and  $(\text{Fe,Cr,Mo})_3\text{O}_4$ . However, referring to the major oxide layer formed in austenitic steels reported by Viswanathan *et al.*, [10] and Wright *et al.*, [21], for simplification and the purposes of this study, the scale is treated as to be all magnetite ( $\text{Fe}_3\text{O}_4$ ). The properties of steam, solid materials, and flue gas from different sources reported by Yeo *et al.*, [22] are used and shown in Table 1.

**Table 1**  
 Properties of steam, solid materials, and flue gas [22].

<i>Inlet steam properties at 35 MPa pressure</i>				
Temperature, °C		600	650	700
Thermal conductivity, W/m °C		0.1169	0.1185	0.1218
Specific heat, J/kg °C		3389	3110	2944
Dynamic viscosity, N s/m <sup>2</sup>		3.59e-05	3.77e-05	3.97e-05
<i>Water wall properties</i>				
Tube material		TP347HFG		
Thermal		23.3		
<i>Fe<sub>3</sub>O<sub>4</sub> iron oxide (magnetite)</i>				
Thermal		0.592 W/m C		
<i>Flue gas composition</i>		<i>Flue gas properties</i>		
Nitrogen,	72.8	Temperature, °C	1200	
Oxygen, mole%	14.0	Dynamics viscosity, N	5.34e-05	
Carbon Dioxide,	2.7	Specific heat, J/kg °C	1323	
Water, mole%	10.5	Thermal conductivity,	0.0879	
<i>Tubes layout (staggered arrangement)</i>				
Gas flow rate, kg/h	400,000			
Number of tube	40			
Transverse pitch, m	2 x OD			
Tube length, m	10			

### 2.3 Simulation procedure

The simulation procedure proposed by Yeo et al. [19] is used in this work. Equations (1) and (2), respectively, are used to determine the metal temperature and scale thickness over a period of time in the boiler tubes. In the absence of the fireside scale formation (refer to Fig. 1), the corresponding denominator variable in Eq. (1) is neglected. The incremental procedures can be summarized as follows [19]:

**Step 1:** The design temperature for the steam is set to  $T_{steam}$  at the inlet of the reheater or superheater tube. In the absence of scale ( $X_0$ ), Eq. (1) is used to determine the average temperature ( $T_{ave1}$ ) that is the temperature on the internal diameter (ID) of the tube for steam-side scale estimation or on the outer diameter (OD) of the tube for fireside scale estimation. Eq. (2) is used to calculate the scale thickness of  $X_{1a}$  and  $X_{1b}$  for the service time of 1 h and 1000 h, respectively (see Table 2) using the average temperature of  $T_{ave1}$ . Subsequently, by subtracting one from the other, the scale increase of  $\Delta X_1 (=X_{1b} - X_{1a})$  is determined and a new scale thickness of  $X_1 (=X_0 + \Delta X_1)$  is obtained.

**Step 2:** A newly calculated steam-side/fireside scale thickness is used to define the radii for steam-side scale/metal interface or/and metal/fireside scale interface. Equation (1) is used to determine the average temperature of  $T_{ave2}$  which is obtained from the average of the temperatures at the ID

of the tube and the steam-side scale/metal interface (for the internal scale estimation) or the average of the temperatures at the OD of the tube and the metal/fireside scale interface (for the external scale estimation). The average temperature of  $T_{ave2}$  is then used to calculate the scale thickness of  $X_{2a}$  and  $X_{2b}$  for the service time of 1000 and 2500 h respectively using Eq. (2). Subsequently, by subtracting one from the other, the scale increase of  $\Delta X_2 (=X_{2b} - X_{2a})$  is determined and a new scale thickness of  $X_2 (=X_1 + \Delta X_2)$  is obtained. Repeat **Step 2** for further estimations until the final step time as presented in Table 2. In the event of spallation of steam-side or fireside scales at the assumed service time, the corresponding ID or ID of the tube is redefined for wall thinning.

### 2.5 Oxide scale strain

The approach used to estimate the critical failure strain in oxide scale is based on the A-OSFD which reported by Schütze et al. [20]. Under the tensile loading, the critical strain equation for through-scale cracking can be written as following [20]

$$\varepsilon_c = \frac{K_{Ic}}{f \cdot E \sqrt{\pi \tilde{c}_0}} \left( \frac{\tilde{c}_0}{\tilde{c}} \right)^{1/2} \quad (3)$$

where  $K_{Ic}$  is Mode I fracture toughness of the oxide as a material constant ( $\text{MPa}\cdot\text{m}^{1/2}$ );  $f$  is geometrical parameter ( $f = 1.12$  for a surface defect of infinite length);  $\tilde{c}$ ,  $\tilde{c}_0$  are size of a physical scale defect (pore, flaw, etc. in  $\mu\text{m}$ ) with  $\tilde{c}_0$  as a value for normalizing the defect size;  $E$  denotes the Young's modulus of the oxide scale (MPa);  $\nu (= 0.29)$  is Poisson's ratio. In the present study, the  $\tilde{c}_0$  is set to  $1 \mu\text{m}$ , and  $K_{Ic}$  and  $E$  are  $1.4 \text{ MPa}\cdot\text{m}^{1/2}$  and  $208000 \text{ MPa}$  [20], respectively.

### 3. Results and Discussions

The calculations demonstrated here are intended to have rough estimations and shall ideally consider the real-time operating parameters for better estimations. Yeo *et al.*, [19] have made comparisons of the estimated oxide scale growth with the actual experimental/testing data from power plants reported by Eurlings *et al.*, [23]. The measurements of steam-side scale thickness were taken from the power plants for four different experiment/test steam loops (5,890 h, 12,000 h, 17770 h, and 23,215 h) under the KOMET 650 joint research project [23]. The estimations and the actual data at  $630^\circ\text{C}$  and  $650^\circ\text{C}$  steam conditions were reported to be in good agreement [19] as shown in Fig. 2.

In the absence of fireside scale formations, the estimations of the steam-side scale growth and temperature increase for the austenitic alloy TP 347HFG with operating steam temperatures of  $520^\circ\text{C}$ ,  $600^\circ\text{C}$  and  $650^\circ\text{C}$  are presented in Fig. 3. It can be seen from Fig. 3, a higher steam temperature operation leads to larger increases in scale growth and metal temperature. Noticeable temperature increase is shown at the  $650^\circ\text{C}$  steam condition, however, it remains showing a tolerable/acceptable trend.

Next, the oxide scale failure diagram is plotted to examine the limit of integrity of the oxide scales. In order to plot the failure diagram correlating the physical defect  $\tilde{c}$  with the scale thickness ( $d$ ), an exfoliation factor of  $\tilde{c}/d$  can be introduced. Figure 4 shows the estimations of the failure strain and growth of magnetite ( $\text{Fe}_3\text{O}_4$ ) over a period of time for different  $\tilde{c}/d$  and steam temperatures. The exfoliation factor of 0.4 is introduced to have a more conservative estimation for the critical failure strain. For given  $\tilde{c}/d$ , greater steam temperatures would lead to a lower limit of

the critical strain. It simply shows that the likelihood of exfoliation would take place at a lower strain. The oxide scale failure diagram would provide a general guidance to the power plant engineers to estimate the critical strains. It is not meant to provide the size or amount of scale exfoliated from the tube.

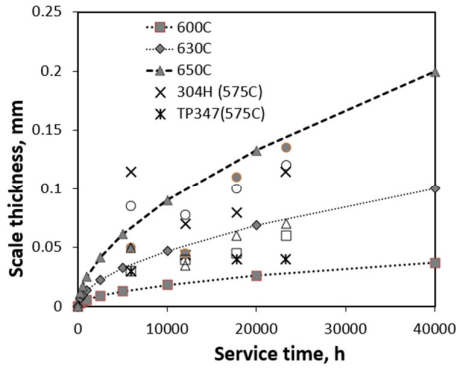


**Fig. 2.** Estimated steam-side oxide scale growths and the actual data (304H and TP347) from the power plants for austenitic alloys [19]

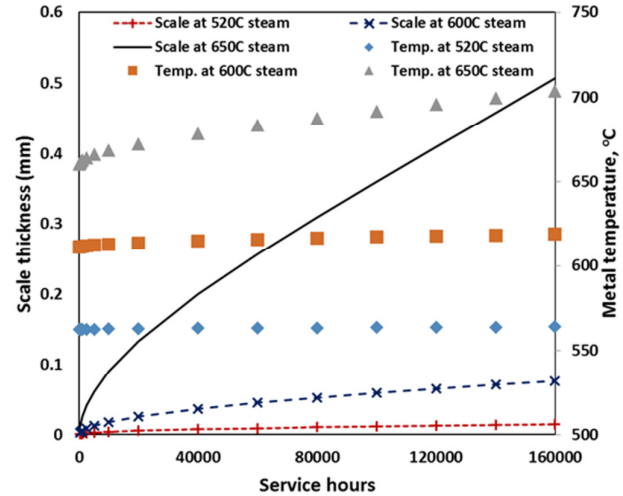


**Fig. 3.** Steam-side oxide scale growth and metal temperature increase

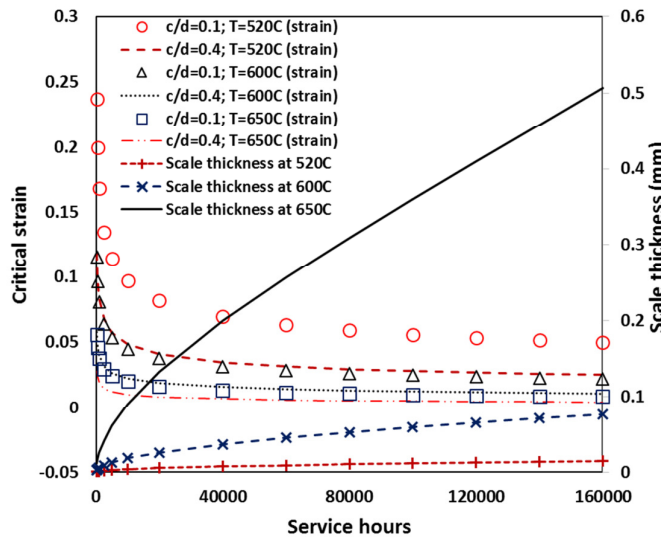


**Fig. 4.** The critical failure strains and scale growths in austenitic tubes for different  $c/d$  and steam temperatures

#### 4. Conclusions

A simple procedure to estimate the oxide scale growths and critical failure strains in boiler tubes over a period of time was presented. Based on the simulations demonstrated here, a higher operation of steam condition would result in a lower critical failure strain in oxide scale to exfoliate. The proposed technique may be of a supplementary condition monitoring tool for evaluating the oxide scale growths and its critical failure strain.

## Acknowledgement

The authors wish to thank Universiti Teknologi Brunei for all the supports.

## References

- [1] Shafiee, S. and Topal, E. "When will fossil fuel reserves be diminished?" *Energy Policy* 37 (2009): 181–189.
- [2] Khattak, M.A., Ashraff, M.A., Ikmal, M., Syafiq, A. and Hazritz, M. "Common types of fuels in steam power plant: a review." *Journal of Advanced Research in Fluid Mechanics and Thermal Sciences* 23 no. 1 (2016): 1-24.
- [3] Beer, J.M. "High efficiency electric power generation: the environmental role." *Progress in Energy Combustion Science* 33, no. 2 (2007): 107–34.
- [4] Pettinau, A., Ferrara, F. and Amorino, C. "Techno-economic comparison between different technologies for a CCS power generation plant integrated with a subbituminous coal mine in Italy." *Applied Energy* 99 (2012): 32–39.
- [5] Franco, A. and Diaz, A. "The future challenges for "clean coal technologies": joining efficiency increase and pollutant emission control." *Energy* 34 (2009): 348–354.
- [6] Zhong, X. Wu, X. and Han, E-H. "The characteristic of oxide scales on T91 tube after long-term service in an ultra-supercritical coal power plant". *The Journal of Supercritical Fluids* 72 (2012): 68-77.
- [7] Viswanathan, R., Coleman, K. and Rao, U. "Materials for ultra-supercritical coal-fired power plant boilers." *International Journal of Pressure Vessels and Piping* 83 (2006): 778-783.
- [8] Armit, J., Holmes, R., Manning, M.I., Meadowcroft, D.B. and Metcalfe, E. (1978). *The Spalling of Steam-Grown Oxide from Superheater and Reheater Tube Steels*. Palo Alto, CA: EPRI.
- [9] Quadackers, W.J., Ennis, P.J., Zurek, J. and Michalik, J. "Steam oxidation of ferritic steels – laboratory test kinetic data". *Materials at High Temperatures* 22, no. 1-2 (2005): 47-60.
- [10] Viswanathan, R., Sarver, J. and Tanzosh, J. "Boiler materials for ultra-supercritical coal power plants—steamside oxidation". *Journal of Materials Engineering and Performance* 15, no. 3 (2006): 255–274.
- [11] Lu, K. "The future of metals", *Science* 328 (2010): 319.
- [12] Weitzel, P.S., "Steam Generator for Advanced Ultra-Supercritical Power Plants 700 to 760C," *ASME 2100 Power Conference*, Denver, CO. July 12-14, 2011.
- [13] Kritzer, P. "Corrosion in high-temperature and supercritical water and aqueous solutions: a review". *The Journal of Supercritical Fluids* 29, no. 1–2 (2004): 1-29.
- [14] Sarver, J.M. and Tanzosh, J. "Steam oxidation testing of candidate ultra-supercritical boiler materials", *The 28<sup>th</sup> International Technical Conference on Coal Utilization and Fuel Systems*, Clearwater, Florida, USA. 9-13 March, 2003.
- [15] Abdullah, A.L, and Yilmaz, F. "Computational analysis of heat transfer enhancement in a circular tube fitted with different inserts." *Journal of Advanced Research in Fluid Mechanics and Thermal Sciences* 40 no. 1 (2017): 59-69.
- [16] Soo, W.Beng. and Japar, W,M,A. Numerical analysis of heat and fluid flow in microchannel heat sink with triangular cavities." *Journal of Advanced Research in Fluid Mechanics and Thermal Sciences* 34 no. 1 (2017): 1-8.
- [17] Nor Azwadi, C.S. and Adamu, I.M. "Turbulent force convective heat transfer of hybrid nano fluid in a circular channel with constant heat flux." *Journal of Advanced Research in Fluid Mechanics and Thermal Sciences* 19 no. 1 (2016): 1-9.
- [18] Wong, M.K., Sheng, L.C., Nor Azwadi, C.S. and Hashim, G.A." Numerical Study of turbulent Flow in Pipe with Sudden Expansion." *Journal of Advanced Research in Fluid Mechanics and Thermal Sciences* 6 no. 1 (2015): 34-48.
- [19] Yeo, W.H., Fry, A.T., Purbolaksono, J., Ramesh, S., Liew, H.L., Inayat-Hussain, J.I. and Hamdi, M. "Oxide scale growth and presumed exfoliation in a 700°C or higher steam condition: A simulation study for future operations of ultra-supercritical power plants". *The Journal of Supercritical Fluids* 92 (2014): 215-222.
- [20] Schütze, M., Tortorelli, P. and Wright, I. "Development of a comprehensive oxide scale failure diagram". *Oxidation of Metals* 73, no. 3-4 (2010): 389-401.
- [21] Wright, I.G. and Dooley, R.B. "A review of the oxidation behavior of structural alloys in steam". *International Materials Review* 55, no. 3 (2010): 129-167.
- [22] Yeo, W.H., Fry, A.T., Ramesh, S., Mohan, R., Liew, H.L., Inayat-Hussain, J.I. and Purbolaksono, J. "Simulating the implications of oxide scale formations in austenitic steels of ultra-supercritical fossil power plants." *Engineering Failure Analysis* 42 (2014): 390-401.
- [23] Uerlings, R., Bruch, U. and Meyer, H. "KOMET 650-Investigations of the operational behavior of boiler materials and their welded joints at temperatures up to 650°C". *VGB Power Tech-International Journal for Electricity and Heat Generation* 3 (2008): 43-49.